iJRASET
International Journal For Research in Applied Science and Engineering Technology

INTERNATIONAL JOURNAL FOR RESEARCH

IN APPLIED SCIENCE & ENGINEERING TECHNOLOGY

Volume: 10 **Issue:** VI **Month of publication:** June 2022

DOI: https://doi.org/10.22214/ijraset.2022.44568

www.ijraset.com

Call: 08813907089 | E-mail ID: ijraset@gmail.com

International Journal for Research in Applied Science & Engineering Technology (IJRASET)
ISSN: 2321-9653; IC Value: 45.98; SJ Impact Factor: 7.538
Volume 10 Issue VI June 2022- Available at www.ijraset.com

Design and Comparative FE Analysis of Connecting Rod

A. K. Yadav[1], K. Ratre[2], B. Biswas[3]
[1]*M. Tech Scholer, Department of Mechanical Engineering, VEC Ambikapur, C.G. India*
[2]*Assiatant Professor, Department of Mechanical Engineering, VEC Ambikapur, C.G. India*
[3]*Assiatant Professor, Department of Mechanical Engineering, VEC Ambikapur, C.G. India*

Abstract: ***The connecting rod is one of the vital transmission parts of the gas engine. One of its functions is to connect the piston and the crankshaft and transmit the force acting on the piston to the crankshaft so that the reciprocating motion of the piston is converted into the rotary motion of the crankshaft, and the external output is done.***
The small end of the connecting rod reciprocates when it works, the big end rotates, and the rod moves in a complex plane, so the force of the connecting rod is very complicated. It is one of the most heavily loaded parts of the gas turbine. The strength of the connecting rod must be checked for the design.
Currently, the calculation methods of the strength of its front generally include the conventional and finite element methods. Compared with the conventional calculation method, the finite element method has the characteristics of high precision and closer to the actual simulation situation.
Keywords: Finite element analysis, Ansys, Design of Solid Model, Connecting Rod, Solid Works 3D Model, Stress Analysis

I. INTRODUCTION

The connecting rod is one of the vital transmission parts of the gas engine.[1] One of its functions is to connect the piston and the crankshaft and transmit the force acting on the piston to the crankshaft so that the reciprocating motion of the piston is converted into the rotary motion of the crankshaft, and the external output is done.
The small end of the connecting rod reciprocates when it works, the big end rotates, and the rod moves in a complex plane, so the force of the connecting rod is very complicated.[1] It is one of the most heavily loaded parts of the gas turbine. When it is working, it is simultaneously subjected to the action of the gas pressure from the piston, the reciprocating inertial force, and the inertial force generated by its swing.[2] The direction changes periodically. In long-term use, the middle l be bent and twisted due to factors such as the piston's violent thrust and the crankshaft's high-speed operation. Once the connecting rod is bent and twisted, in addition to causing the piston to pull the cylinder, it will also cause abnormal wear and tear of the piston, gas, cylinder crankshaft, and other parts, and it is easy to cause fatigue damage and breakage, resulting in engine failure. It is related to the safety of users, causing severe damage.
It has become difficult for designers to create more benefits for the enterprise.[3] When the engine bore is enlarged, the power will increase. Whether the bearing capacity of the original structure meets the requirements will become a critical link. The "design-validation-design" model in the conventional design method in the past cannot meet the requirements of the fierce market competition due to the significant investment and long verification period.
The finite element method should be used in the design process, which can improve the design efficiency and only need to carry out the necessary FEA tests in the final stage, dramatically improves the work efficiency, accelerates the speed of product development of the enterprise, and improves the market competitiveness of the enterprise while improving the scientific research ability of the enterprise.
The conventional connecting rod design involves the dynamic characteristics, but with the development trend of the engine's high speed and high power, the static design cannot meet the needs more and more. For example, a specific engine connecting rod is considered to have sufficient strength when performing static strength checks and finite element static calculations.[4] However, the 200-hour engine bench strengthening test and the 20,000-kilometer road test of the whole vehicle was found many times that the whole vehicle and the whole vehicle had sufficient strength. The engine has abnormal noise and constant motion, and in recent years, it has been found that the motorcycle products should have cracks in them, which is a fatal damage phenomenon.[5] Therefore, studying the dynamic characteristics of the connecting rod from the viewpoint of modern design has become essential in its design.

ISSN: 2321-9653; IC Value: 45.98; SJ Impact Factor: 7.538
Volume 10 Issue VI June 2022- Available at www.ijraset.com

II. SOLID MODELING AND DESIGN CALCULATION

Classical elastic mechanics obtains its analytical solutions by solving differential equations. The finite element method avoids solving differential equations so that the finite element method can solve engineering problems with complex shapes, structures, and boundary conditions. It replaces the design-verification-design cycle in the conventional design method: the parametric design and feature modelling technology to build a 3D solid model. 3D contact finite element analysis method analyzes the bolts, body, and cap. Its Big end assembly composed of bearing bush has been subjected to the nonlinear calculation under the action of the maximum tensile load. The three-dimensional finite element method analyzes the modal distribution of its dynamic characteristics and the mode shape of each mode and points out its weak link. Feature-based modelling technology builds three-dimensional solids and models and establishes a three-dimensional Model.

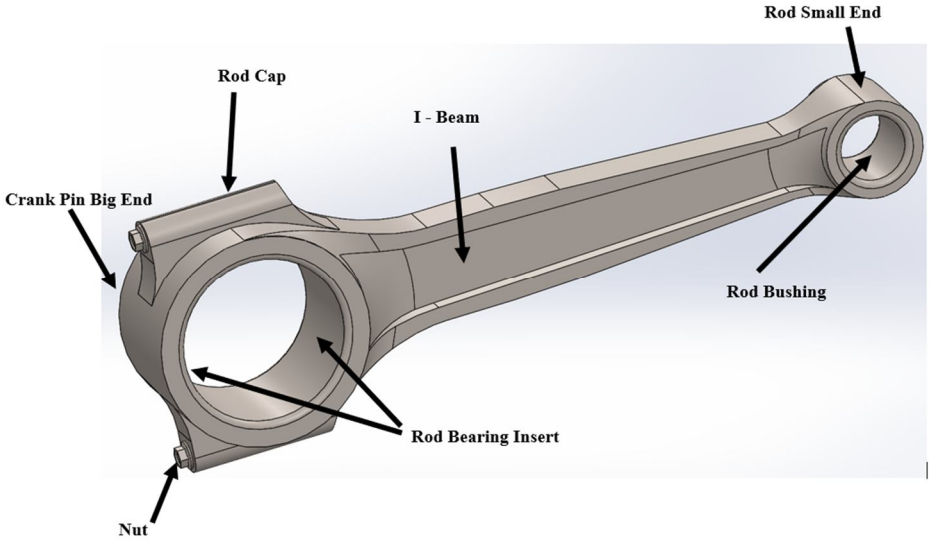

Figure 1: Connecting Rod Solid Model

A. The theoretical basis of the finite element method

The boundary conditions determine the constraint boundary conditions for the rigid body displacement constraints of the connecting rod (including bolts, bearing bushes, and bushings) according to the analyzed problems and models. Different models use different constraints. When examining the deformation of the inner hole surface of the big end of the connecting rod, the inner hole surface of the small end is generally fully restrained. When examining the deformation, since the big end hole relates to the crank pin, one end face connected to the crank pin is fully constrained, the other end face can move in the axial direction, and the displacement coordination constraint is carried out at a node at the top of the small end.[6] The finite element analysis considers the influence of boundary conditions such as bearing length and elastic deformation. The elastic deformation was restoring force describes the preload load, which can more accurately reflect the change and influence of the large and small bolt preload loads. The connecting rod bearing assembly preload acts in the form of surface force on the contact surface; the inertial load is applied to the small end of it according to the cosine distribution law; the maximum burst pressure is applied to the small end of the connecting rod according to the cosine distribution law. The integral three-dimensional finite element analysis of the diesel Engine connecting rod, in which the force state of the connecting rod was fixed now of the worst working condition, and it was converted into a static force for division. In the analysis and simulation calculation, the connecting rod is regarded as a two-force rod; and the centre of the crank pin is fixed and restrained, the line exerts a load on the piston pin, and the constraint force of the crank pin is the same as that of the piston pin.

Numerical simulation technology is one of the fundamental driving forces for the formation and development of modern engineering. First, the numerical simulation methods commonly used in the engineering field include finite element, typical boundary element, usual discrete element method, and finite difference method, and the conventional element method is the most widely used one among them.

Based on element analysis, each element is assembled into a whole structure by using equilibrium conditions and continuous conditions. Divide the whole under the condition of determining the boundary and analyze it to obtain the whole parameter relationship equation system, that is, the matrix equation.

B. Constant strain tetrahedral elements

The constant-strain 4-node tetrahedral element is better for calculating object shape adaptability in spatial problem pairs, and the higher tetrahedral element is less commonly used.

1) Displacement Function

The tetrahedral element 4 has vertices i, j, m, and l as nodes. Each node has three degrees of freedom, and an element has 12 degrees of freedom, so the displacement function given by generalized coordinates is linear,

$$U = \varphi\beta = \begin{bmatrix} \emptyset & 0 & 0 \\ 0 & \emptyset & 0 \\ 0 & 0 & \emptyset \end{bmatrix}_{\beta} \tag{1.1}$$

Where:

$$\emptyset = [1 \quad x \quad y \quad z]$$
$$\beta = [\beta_1\beta_2\beta_3 \dots\dots\dots\dots\beta_{12}]$$

Substitute the coordinates of the four nodes into the formula to get.

$$\widetilde{a^e} = \begin{bmatrix} \tilde{A} & 0 & 0 \\ 0 & \tilde{A} & 0 \\ 0 & 0 & \tilde{A} \end{bmatrix}\beta = A\beta \tag{1.2}$$

Among

$$\widetilde{a^e} = [u_1 \quad u_2 \quad u_3 \quad u_4 \quad v_1 \quad v_2 \quad v_3 \quad v_4 \quad w_1 \quad w_2 \quad w_3 \quad w_4]^T$$
$$\tilde{A} = \begin{bmatrix} 1 & x_i & y_i & z_i \\ 1 & x_j & y_j & z_j \\ 1 & x_m & y_m & z_m \\ 1 & x_l & y_l & z_l \end{bmatrix} \tag{1.3}$$

The generalized coordinates are obtained by formula (1.3) and then substituted into formula (1.1).

$$u = N_i u_i + N_j u_j + N_m u_m + N_l u_l$$
$$v = N_i v_i + N_j v_j + N_m v_m + N_l v_l$$
$$w = N_i w_i + N_j w_j + N_m w_m + N_l w_l \tag{1.4}$$

in the formula

$$\begin{cases} N_i = \frac{1}{6V}(a_i + b_i x + c_i y + d_i z) \\ N_j = \frac{1}{6V}(a_j + b_j x + c_j y + d_j z) \\ N_m = \frac{1}{6V}(a_m + b_m x + c_m y + d_m z) \\ N_l = \frac{1}{6V}(a_l + b_l x + c_l y + d_l z) \end{cases} \tag{1.5}$$

Among

$$a_i = \begin{vmatrix} x_j & y_j & z_j \\ x_m & y_m & z_m \\ x_l & y_l & z_l \end{vmatrix} \quad b_i = \begin{vmatrix} 1 & y_j & z_j \\ 1 & y_m & z_m \\ 1 & y_l & z_l \end{vmatrix}$$

$$c_i = \begin{vmatrix} 1 & x_j & z_j \\ 1 & x_m & z_m \\ 1 & x_l & z_l \end{vmatrix} \quad d_i = \begin{vmatrix} 1 & x_j & y_j \\ 1 & x_m & y_m \\ 1 & x_l & y_l \end{vmatrix} \tag{1.6}$$

$$V = \frac{1}{6}\begin{vmatrix} 1 & x_i & y_i & z_i \\ 1 & x_j & y_j & z_j \\ 1 & x_m & y_m & z_m \\ 1 & x_l & y_l & z_l \end{vmatrix} \tag{1.7}$$

V is the volume of the tetrahedron (i j m l). For the volume of the tetrahedron to be non-negative, the numbering of the element nodes i, j, m, and l must be in a particular order. In the right-handed coordinate system, when turning in the direction i → j → m → l, the right-handed helix should advance in the direction l.

From equation (1.7), the matrix of unit displacement is expressed as:

$$U = \begin{Bmatrix} u \\ v \\ w \end{Bmatrix} = Na^e = \begin{bmatrix} IN_i & IN_j & IN_m & IN_l \end{bmatrix} a^e \quad 1.8$$

$$a^e = \begin{bmatrix} u_i & v_i & w_i & u_j & v_j & w_j & u_m & v_m & w_m & u_l & v_l & w_l \end{bmatrix}^T$$

Where: "I" is the third-order identity matrix.
Since the displacement function is linear, the displacement at the interface between adjacent elements is continuous, and all constant strain tetrahedra

2) Strain Matrix

In spatial problems, each point has 6 strain components:

$$\varepsilon = \begin{bmatrix} \varepsilon_x & \varepsilon_y & \varepsilon_z & \gamma_{xy} & \gamma_{yz} & \gamma_{zx} \end{bmatrix}^T$$

$$= \left\{ \frac{\partial u}{\partial x} \frac{\partial v}{\partial y} \frac{\partial w}{\partial z} \quad \frac{\partial u}{\partial y} + \frac{\partial v}{\partial x} \quad \frac{\partial v}{\partial z} + \frac{\partial w}{\partial y} \quad \frac{\partial w}{\partial x} + \frac{\partial u}{\partial z} \right\}^T \quad 1.9$$

Substituting the value from eq.1.9 into the formula, we get

$$\varepsilon = Ba^e = \begin{bmatrix} B_i & -B_j & B_m & -B_l \end{bmatrix} a^e \quad 1.10$$

Each block matrix of the strain matrix B is a 6×3 matrix as:

$$B_r = \frac{1}{6V} \begin{bmatrix} b_r & 0 & 0 & c_r & 0 & d_r \\ 0 & c_r & 0 & b_r & d_r & 0 \\ 0 & 0 & d_r & 0 & c_r & b_r \end{bmatrix}^T \quad 1.11$$

$r = i, j, m, l$

The strain matrix B is a constant matrix, and the strain component in the element is also constant.

3) Element stiffness matrix

Substituting the strain matrix B of formula 1.11 into the general formula, since the strain matrix is a constant, the calculation is simple

$$K^e = \int B^T D B \; dV = B^T D B V \quad 1.12$$

Express the element stiffness matrix in the form of nodal blocks as

$$K^e = \begin{bmatrix} K_{ii} & K_{ij} & K_{im} & K_{il} \\ K_{ji} & K_{jj} & K_{jm} & K_{jl} \\ K_{mi} & K_{mj} & K_{mm} & K_{ml} \\ K_{li} & K_{lj} & K_{lm} & K_{ll} \end{bmatrix} \quad 1.13$$

Where block K_{r5}(3x3) is given by the following formula.

$$B^T D B V = \frac{E(1-v)}{36V(1+v)(1-2v)} \begin{bmatrix} K_1 & K_4 & K_7 \\ K_2 & K_5 & K_8 \\ K_3 & K_6 & K_9 \end{bmatrix} \quad 1.14$$

(r, s = i, j, m, l)

Tetrahedral elements have a strong ability for boundary fitting, but the division of elements is complicated and prone to errors. The high tetrahedron unit, which is not commonly used, will not be introduced here.

4) Hexahedral Element

For the eight-node hexahedral element shown in Figure 2, the overall coordinates of its eight nodes 1, 2, ..., 8 are (x, y, z), (x2, y2, z2), …….. (x8, y8, z8).
Figure 3 shows the corresponding cubic element at local coordinates (ξ, η, ζ) with side length 2 and origin at the centre. Take the displacement interpolation function as

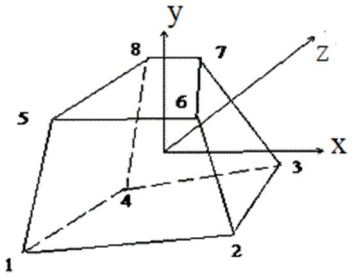

Figure 2: Eight nodes hexahedral element

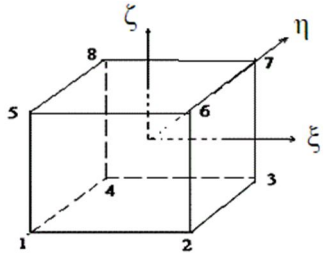

Figure 3: cubic element at local coordinates

$$u = a_1 + a_{2\xi} + a_{3\eta} + a_{4\zeta} + a_{5\xi\eta} + a_{6\eta\zeta} + a_{7\zeta\xi} + a_{8\xi\eta\zeta} \quad 1.15$$

Substitute the displacement values ui (i =1, 2,……8) of the eight nodes into the above formula, and the expression of the displacement interpolation function can be obtained,

$$u = \sum_{i=1}^{8} N_i u_i \quad 1.16$$

It is reasonable to obtain expressions for the other two displacement interpolation functions:

$$v = \sum_{i=1}^{8} N_i v_i \quad 1.17$$

$$w = \sum_{i=1}^{8} N_i w_i \quad 1.18$$

shape function,

$$N_i = \frac{1}{8}(1 + \xi,\xi)(1 + \eta,\eta)(1 + \zeta,\zeta), \quad (i=1,2,\ldots\ldots\ldots 8) \quad 1.19$$

Write the displacement interpolation function in the matrix form we get.

$$[f] = [N]^e[\delta]^e \quad 1.20$$

Where;

$$[N]^e = \begin{bmatrix} N_1 & 0 & 0 & N_2 & 0 & 0 & \ldots & N_8 & 0 & 0 \\ 0 & N_1 & 0 & 0 & N_2 & 0 & \ldots & 0 & N_8 & 0 \\ 0 & 0 & N_1 & 0 & 0 & N_2 & \ldots & 0 & 0 & N_8 \end{bmatrix}$$

The local coordinates of the eight nodes of the element are.

(ξ1, η1, ζ1) = (-1, -1, -1)
(ξ2, η2, ζ2) = (1, -1, -1)
(ξ3, η3, ζ3) = (1, 1, -1)
(ξ4, η4, ζ4) = (-1, 1, -1)
(ξ5, η5, ζ5) = (-1, -1, 1)
(ξ6, η6, ζ6) = (1, -1, 1)
(ξ7, η7, ζ7) = (1, 1, 1)
(ξ8, η8, ζ8) = (-1, 1, 1)

According to the method of iso parametric element unit, from the coordinate transformation formula,

$$\begin{cases} x = \sum_{i=1}^{8} N_i x_i \\ y = \sum_{i=1}^{8} N_i y_i \\ z = \sum_{i=1}^{8} N_i z_i \end{cases} \quad 1.21$$

Using the coordinate transforming equation (1.21), the eight-node regular hexahedron element can be transformed into any prismatic hexahedron element.

C. Finite Element Method In Practical Calculation

The finite element method is a numerical calculation method for solving mathematical equations. It regards the solution area as consisting of many interconnected subdomains at small nodes, and its model gives approximate solutions to the subdomains of the fundamental equations because the subdomains can be divided into different sizes of various shapes and sizes, so it adapts well to complex geometries, material properties, and boundary conditions. The following takes the rigid space frame as an example to introduce how the method with the element is applied to the actual calculation.

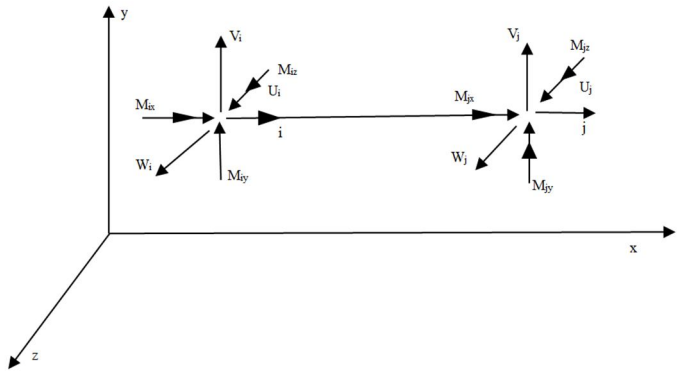

Figure 4: nodal forces of the spatial rigid frame element

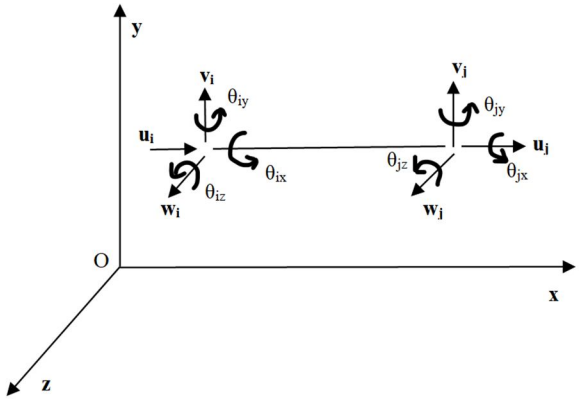

Figure 5: Nodal Displacement of Spatial Rigid Frame Elements

The axis of the member is selected as the x-axis, and the other two coordinate axes are selected as the central axis of the centroid of the section. Figure 4 shows the element node and its positive direction, and Figure 5 shows the element node position and positive direction. According to the solution of the element stiffness matrix of the rigid plane frame and the unit torsion angle generated at one end of the fixed rod at both ends, the element stiffness matrix of the rigid space frame is,

Let (xx, xy, xz), (yx, yy, yz), and (zx, zy, zz) be the direction cosines of the three axes x, y, z in the Oxyz coordinate system, respectively, to obtain the vector change matrix R

$$R = \begin{bmatrix} x'_x & x'_y & x'_z \\ y'_x & y'_y & y'_z \\ z'_x & z'_y & z'_z \end{bmatrix} \quad 1.23$$

With the vector coordinates transformation formula, the coordinate transformation matrix T of the nodal force or nodal displacement of the rigid space frame can be constructed.

$$T = \begin{bmatrix} R & & & \\ & R & & \\ & & R & \\ & & & R \end{bmatrix}$$

This space rigid frame element stiffness matrix coordinate change formula is

$$\overline{K^e} = T^T K^e T$$

Where:

$\overline{K^e}$ = element stiffness matrix in the global coordinate system

K^e = element stiffness matrix in the local coordinate system

The non-nodal loads are decomposed along the local coordinate axes x, y, z, and then the fixed-end reaction is calculated. At this time, attention should be paid to the sign of the fixed-end reaction force in the local coordinate axis. Finally, these fixed-end reaction forces are transformed to the $\overline{x}$, $\overline{y}$, $\overline{z}$ Directions of the overall coordinate axis through coordinate transformation and a minus sign are added before it to be the equivalent nodal load.

III. MOTION AND FORCE ANALYSIS OF CONNECTING ROD

In the kinematics calculation of the crank connecting rod mechanism, the movement of the middle crank can be approximated as a constant speed rotation, which is entirely acceptable for a high-speed engine, because when the engine works in a stable condition, due to the unevenness of the pinch torque The resulting change in the crank rotation angular velocity is not large. The reason for this is that the angular velocity of the crank in this crank-link machine is,

$$\omega = \frac{\pi n}{30} \text{ radians/sec}$$

Where n is the rotational speed of the crank, r/min

TABLE 1
MAIN PARAMETERS OF CONNECTING ROD

Mass of connecting rod assembly (m_r)	108g
Mass weight of piston group (m_p)	110g
Maximum burst pressure of the gas (P)	54 bars
Rated rotational speed of crankshaft (n)	8500 rpm
The distance from the centre of mass of the connecting rod to the centre of the Big end hole (L_2)	29mm
The radius of gyration of a crankshaft (R)	24.75mm
cylinder diameter (D)	47mm

A. Stress Calculation Of Connecting Rod Under Compression

The P' value in the dynamic calculation can be regarded as the maximum compressive load of the connecting rod, and it is approximately considered that the load of the connecting rod at the top dead centre of the expansion stroke is:

$$P_{c\,max} = \frac{\pi}{4} D^2 P_z - \frac{G_j}{g} R\omega^2(1+\lambda) \quad (N) \quad 2.16$$

Where:
D = cylinder diameter (mm)
R = Shank Radius (mm)
Gj = The weight of the reciprocating motion of the piston connecting rod group (N)
Pz = The highest burst pressure of the gas in the cylinder (N/mm2)
ω = Crankshaft Rotation Angular Velocity (1/s)
λ = connecting rod length, λ=R/L
L = Centre between Big and small end holes of connecting rod (mm)
g = force acceleration, (mm/s2)
Substitute the data to calculate,

$$P_{c\,max} = 6622\ N$$

When the connecting rod is under compression, it is equivalent to compression. In addition to the compressive stress on the rod body, there is an additional longitudinal bending stress. There is no internal support and additional longitudinal bending stress in the swing plane of the connecting rod and its vertical plane. This practical term shows that the additional longitudinal bending stress is proportional to the ratio of the load to the critical load of the compression bar.

B. Stress Calculation Of Connecting Rod Under Tension

The maximum tensile load that the connecting rod bears are the minimum value Pc of the connecting rod force PC in the dynamic calculation, or the maximum reciprocating inertial force of the movable connecting rod group at the top dead centre, and the tensile stress generated in the rod body is $\sigma_{min} = \frac{P_{c\,min}}{f_c}\ (N/mm^2)$ available $P_{c\,min} = -\frac{G_j}{g}\ R\omega^2\ (1 + \lambda)$

By solving the above calculation, Substitute data into the equation
$P_{c\,min}$= -2742 N, then use the values of σ_a, and σ_m (Table 2) to calculate the safety factor for fatigue.

TABLE 2
STRESS AND AMPLITUDE MEAN STRESS OF CONNECTING ROD BODY

stress	A plane	B plane
Stress amplitude σ_a	$\frac{\sigma_{x\,max} - \sigma_{min}}{2}$	$\frac{\sigma_{y\,max} - \sigma_{min}}{2}$
mean stress σ_m	$\frac{\sigma_{x\,max} - \sigma_{min}}{2}$	$\frac{\sigma_{y\,max} - \sigma_{min}}{2}$

IV. FINITE ELEMENT ANALYSIS OF STATIC STRENGTH OF CONNECTING RODS

The requirements for the calculation model must first have a certain degree of accuracy, and secondly, the calculation model must have a good economy. The simplified calculation model must accurately reflect the structure's actual situation. Otherwise, the structure's finite element calculation results will have no practical significance. When establishing a calculation model, a complex calculation model has high accuracy.

Appropriate selection should be based on calculation accuracy, mesh generation, and simulated boundary conditions. The solid model of the connecting rod meshes with a 10-node tetrahedral element type, and the global element size is defined as 2 according to the needs, and the mesh is refined in a place where it is easy to deform and break. The 10-node element SOLID92 is used in this paper, the number of grids is 24,787, and the number of nodes is 43,364. The model is shown in Figure 6.

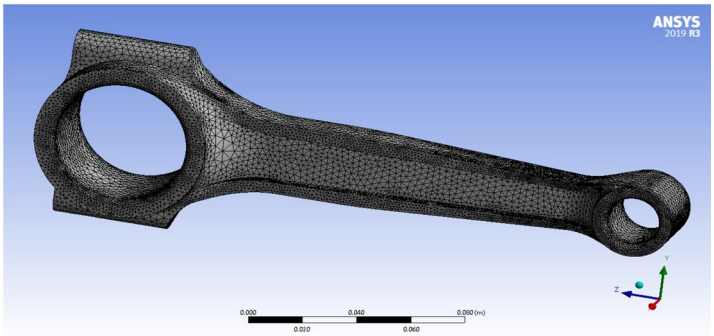

Figure 6: Finite element model of connecting rod

TABLE 3:
20 CRMNMO MATERIAL PROPERTIES

Material name	Elastic Modulus	Poisson's ratio (μ)	mass density (kg/m^3)	σ_b (MPa)	σ_x (MPa)	σ_{-1} (MPa)
20CrMnMo	2.1e11	0.3	7. 8e3	1080	785	450

A. Stress Analysis Under Compression Conditions

1) Big-end Strength Analysis

Figure 7-9 shows the stress profile and deformation diagram of the small end of the connecting rod and the big end under the compression condition. Under compression, the maximum stress value of the big end is 386MPa. The seat is at the transition fillet between the big end and the shaft, close to the centre position and the actual situation. The deformation of the big end of the connecting rod is shown in Figure 9, and the maximum displacement is 0.0852mm. Because the small end is fixed, the force value of the small end is small at this time, and the position of the rod body close to the big end is still a critical section.

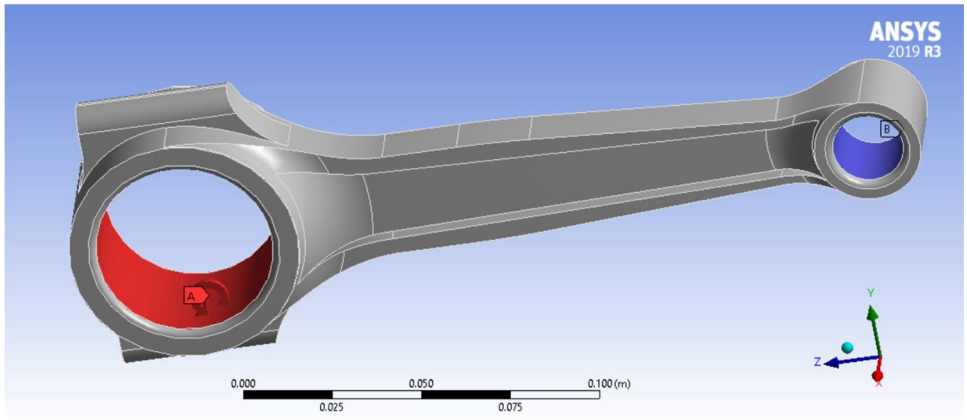

Figure 7: Constraints and loads under compression at the Big end

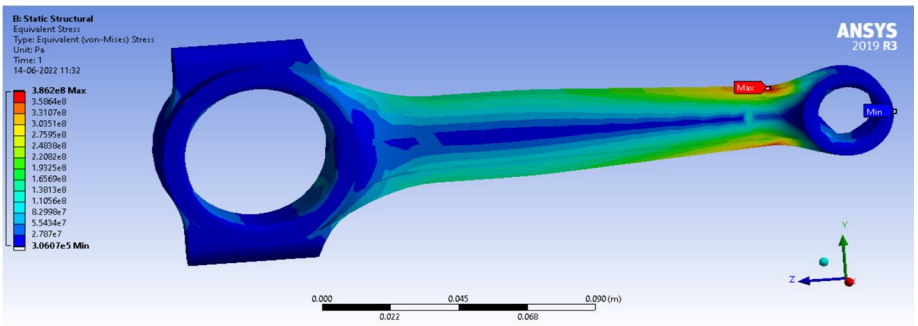

Figure 8: The stress distribution profile diagram of the large end under the condition of compression

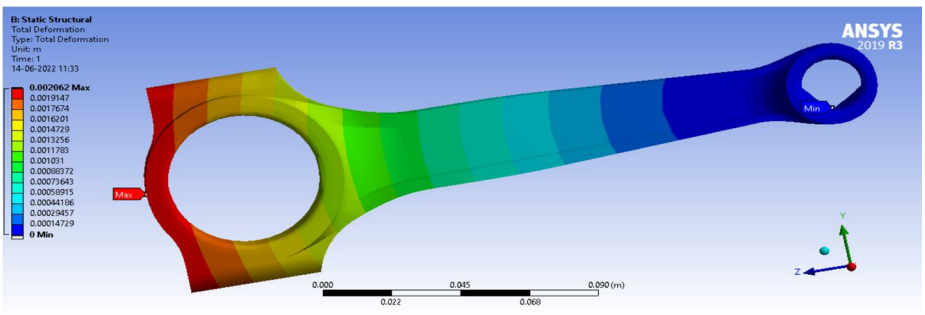

Figure 9: Deformation profile diagram under the condition of compression at the big end

B. Small end Strength Analysis

Figure 10-12 shows the stress and deformation diagram of the connecting rod's big-end and the connecting rod's small end under the compression condition. Under the compression condition, the maximum stress value of the small end is 497 MPa, located at the transition fillet between the big end and the shaft. Close to the centre. At the same time, the position of the small end near the 45o section and the transition fillet between the small end of the connecting rod and the shaft are high-stress areas, which should also be the focus of the experimental investigation. The deformation of the small end of the connecting rod is shown in Figure 10, and the maximum displacement is 0.0283mm.

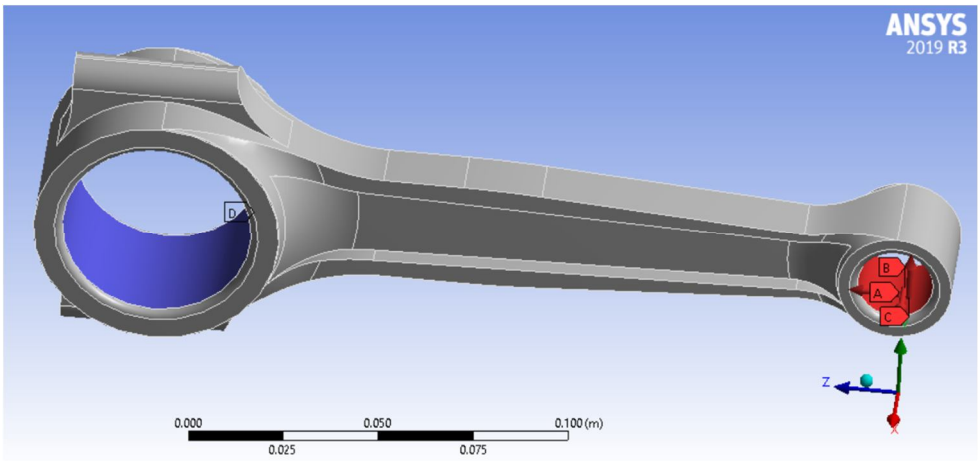

Figure 10: Constraints and loads under compression at Small end

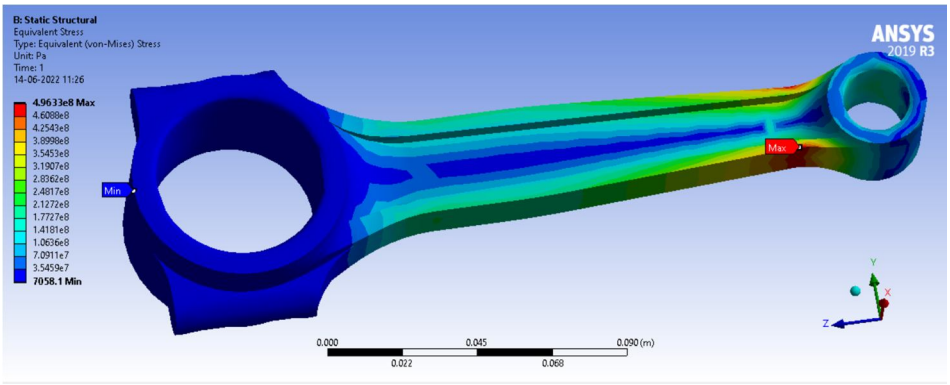

Figure 11: Stress distribution profile diagram under the condition of small end under compression

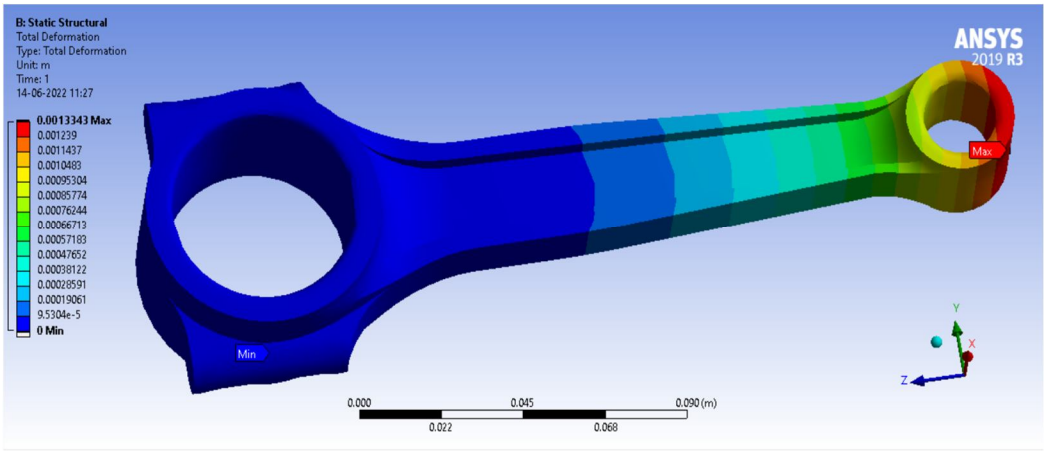

Figure 12: Deformation profile diagram under the condition of small end under compression

C. Stress Analysis Under Tensile Condition

1) Big-End Strength Analysis

Figure 13-15 shows the stress cloud diagram and deformation diagram of the small end of the connecting rod and the big end under the tensile condition. Under the tensile condition, the maximum stress value of the big end is 104 MPa, located inside the big end hole. Meanwhile, near 90° on the big end. The section location and the transition fillet between the big end of the connecting rod and the shaft are high-stress areas. The deformation of the big end of the connecting rod is shown in Figure. 15, and the maximum displacement is 0.0135mm

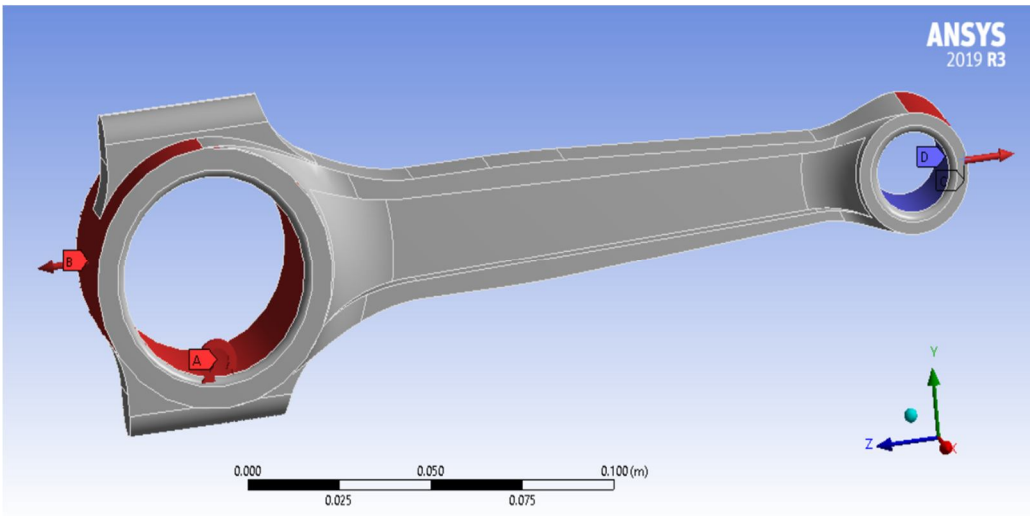

Figure 13: Constraints and loads at the big end in tension

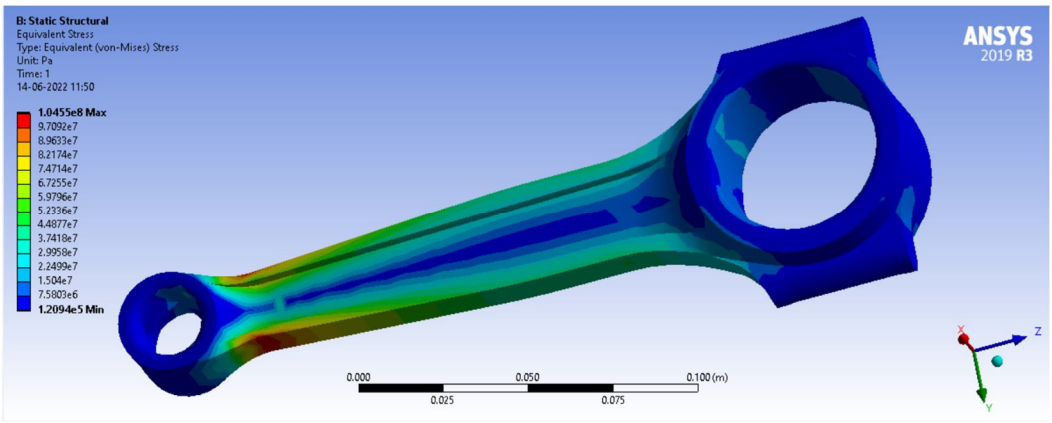

Figure 14: The stress distribution profile diagram under the tension condition of the big end

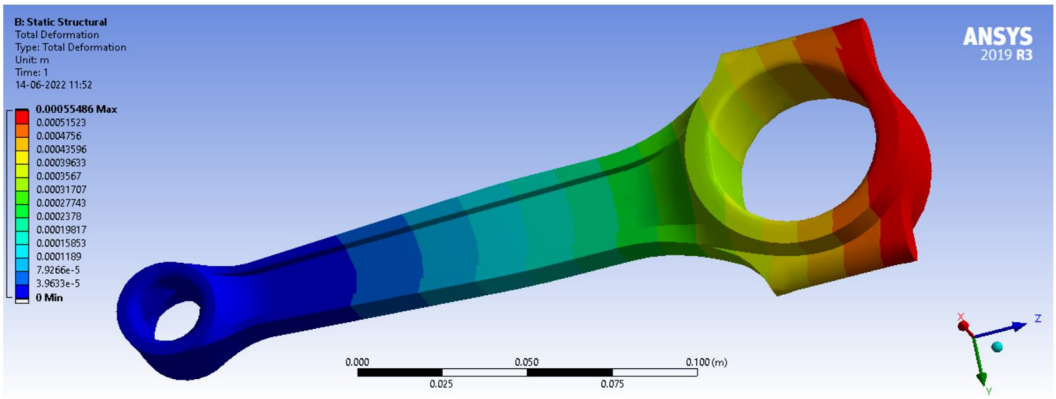

Figure 15: Deformation profile diagram of the large end under tension

2) Small end Strength Analysis

Figure 16-18 shows the stress diagram and deformation diagram of the large end of the connecting rod and the small end under the tensile condition. Under the tensile condition, the maximum stress value of the small end is 16-0 shrimp a, which is located near the oil hole of the small end hole of the connecting rod: meanwhile, in the Small end near 45. The high seat force area is the cross-section position and the transition fillet between the big end of the connecting rod and the shaft. The deformation of the small end of the connecting rod is shown in Figure 18, although the large displacement is 0.0144mm.

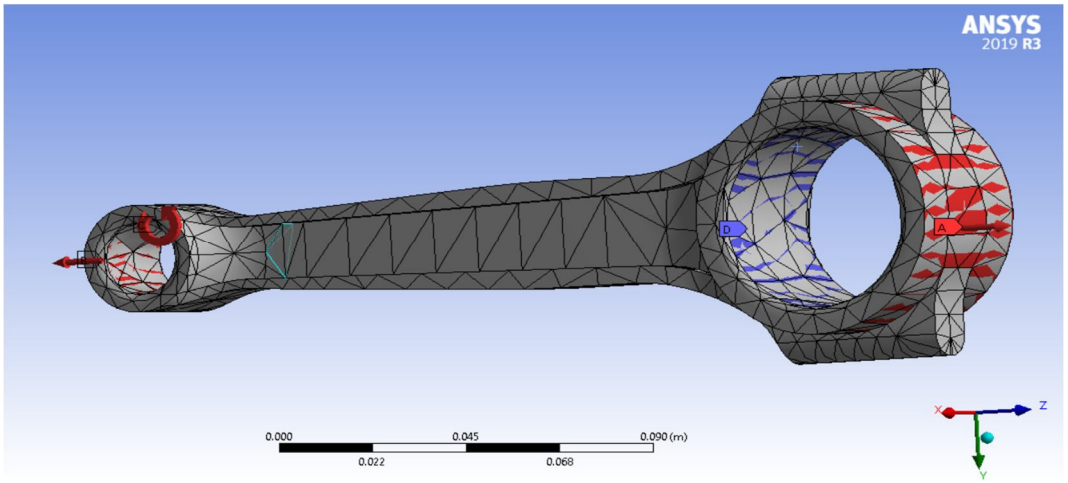

Figure 16: Constraints and loads for small end in tension

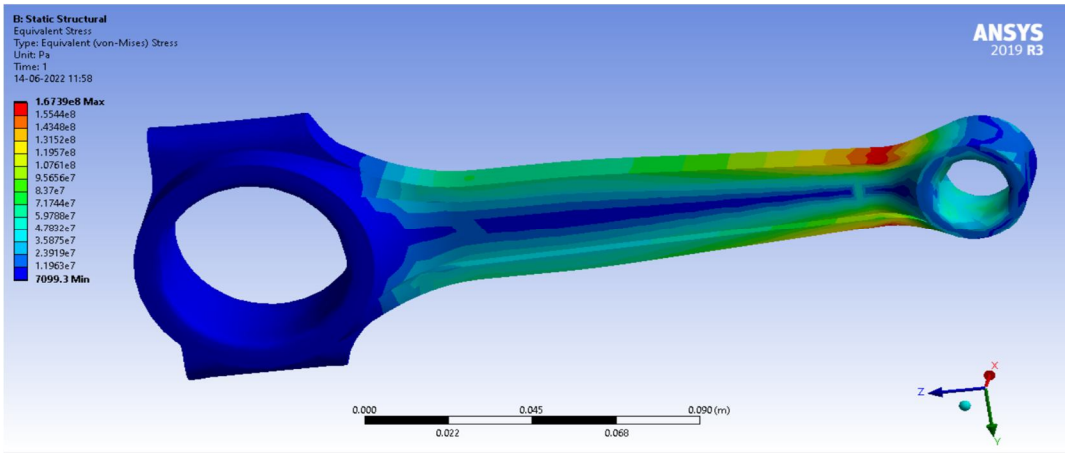

Figure 17: Stress distribution profile diagram under the tension condition of the small end

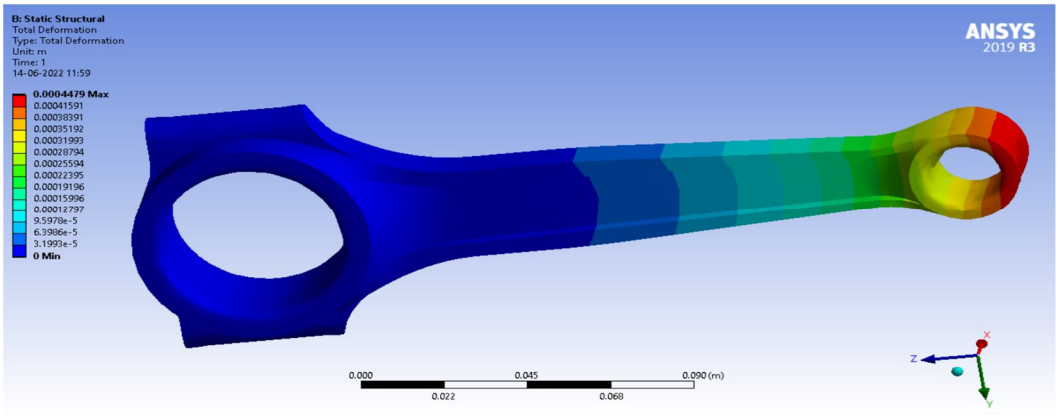

Figure 18: Deformation of the small end under tension

It can be seen from the cloud diagram provided by ANSYS after the stress calculation that the stress concentration is at the transition between the large end of the connecting rod and the shaft and the small end of the connecting rod and the shaft. This is consistent with the actual situation. The calculation result obtains the stress distribution cloud diagram of the connecting rod and analyzes the dangerous parts.

In the maximum tension condition, it can be seen from the figure 17 that the maximum stress of the connecting rod is 167.52Mpa, and the safety factor is close to 6.5, so the tensile strength of the connecting rod is sufficient; in the maximum compression condition, the stress at the small end of the connecting rod is 539.59Mpa, the stress at the transition fillet is 403-488 MPa, and the safety factor is about 1.5. The compressive strength of this connecting rod also basically meets the requirements.

From the post-processing displacement and isochromatic strain diagrams, it can be known that the deformation of the connecting rod is in tension and compression. Compared with the axial clearance between the connecting rod and the piston specified in the technical manual, the value is within the allowable range.

TABLE 4
COMPARISON OF RESULTS BETWEEN THE CONVENTIONAL METHOD AND FINITE ELEMENT METHOD

		conventional calculation method	Finite Element Method	reduction ratio
Under Compression	Big end	437.38 MPa	386.17 MPa	13.26 %
	Small end	539.59 MPa	496.54 MPa	8.67 %
Under Tension	Big end	116.09 MPa	104.26 MPa	11.35 %
	Small end	183.57 MPa	167.52 MPa	9.58 %

Table no 4 compares the conventional method of connecting rod and the finite element calculation method. Since this model has not been tested, the accuracy of the calculation results cannot be correctly measured, but from the comparison results calculated by similar models, it can be seen that the connecting rods with the same structural size have the same strength as the connecting rods based on the finite element method. The calculated value is slightly smaller than that of the conventional calculation method.

V. CONCLUSION

In this paper, the performance of the engine connecting rod produced by our factory is analyzed by ANSYS software, and the static strength and modal characteristics of the connecting rod are obtained, which provides an improved basis for the low vibration and structural strength of this model and has a certain reference value for the calculation of the strength of the engine connecting rod in the future. Although the research on this subject has achieved certain results, each method has shortcomings, and some content related to this subject needs further development. The following is the prospect for this subject: The engine connecting rod is an important part of connecting the piston and the crankshaft. It is subjected to alternating loads such as bar, compression, and bending during operation. Therefore, high requirements for its rigidity and strength are put forward, which is the focus of engine design. One of the difficulties. The research on the connecting rod involves many theories and disciplines. This paper only does some preliminary work. Many problems that are too close to the actual displacement and load constraints need further research.

REFERENCES

[1] J. Zhang, “Finite Element Analysis of EA 113 Gasoline Engine Connecting Rod,” Int. J. Mech. Eng. Appl., vol. 5, p. 208, Jan. 2017, doi: 10.11648/j.ijmea.20170504.14.
[2] I. Kaymaz and C. A. McMahon, “A probabilistic design system for reliability-based design optimization,” Struct. Multidiscip. Optim., vol. 28, no. 6, pp. 416–426, 2004, doi: 10.1007/s00158-004-0444-6.
[3] W. Helal, W. Zhang, X. Li, and G. Wang, “A Study on the Fatigue Strength of a Low-Speed Diesel Engine Connecting Rod Made of 42CrMoA,” Int. J. Eng. Res. Africa, vol. 49, pp. 139–151, Jun. 2020, doi: 10.4028/www.scientific.net/JERA.49.139.
[4] S. Y. Lee, S. B. Lee, H. S. Kim, T. G. Kim, M. G. Kam, and J. W. Yoon, “Failure Analysis of Connecting Rod at Big End,” Key Eng. Mater., vol. 306–308, pp. 345–350, 2006, doi: 10.4028/www.scientific.net/kem.306-308.345.
[5] G. Wang, X. Li, L. Guo, and J. Ma, “Strength Calculation Analysis of Diesel Engine Linkage Based on Three-Dimensional Contact Finite Element Method,” Appl. Mech. Mater., vol. 148–149, pp. 1202–1208, Dec. 2011, doi: 10.4028/www.scientific.net/AMM.148-149.1202.
[6] J. Liu, S. Kou, and D. He, “Comparative analysis of the fracture splitting deformation of the big end for C70S6, 36MnVS4 and 46MnVS5 connecting rods,” IOP Conf. Ser. Mater. Sci. Eng., vol. 772, p. 12113, Mar. 2020, doi: 10.1088/1757-899X/772/1/012113.

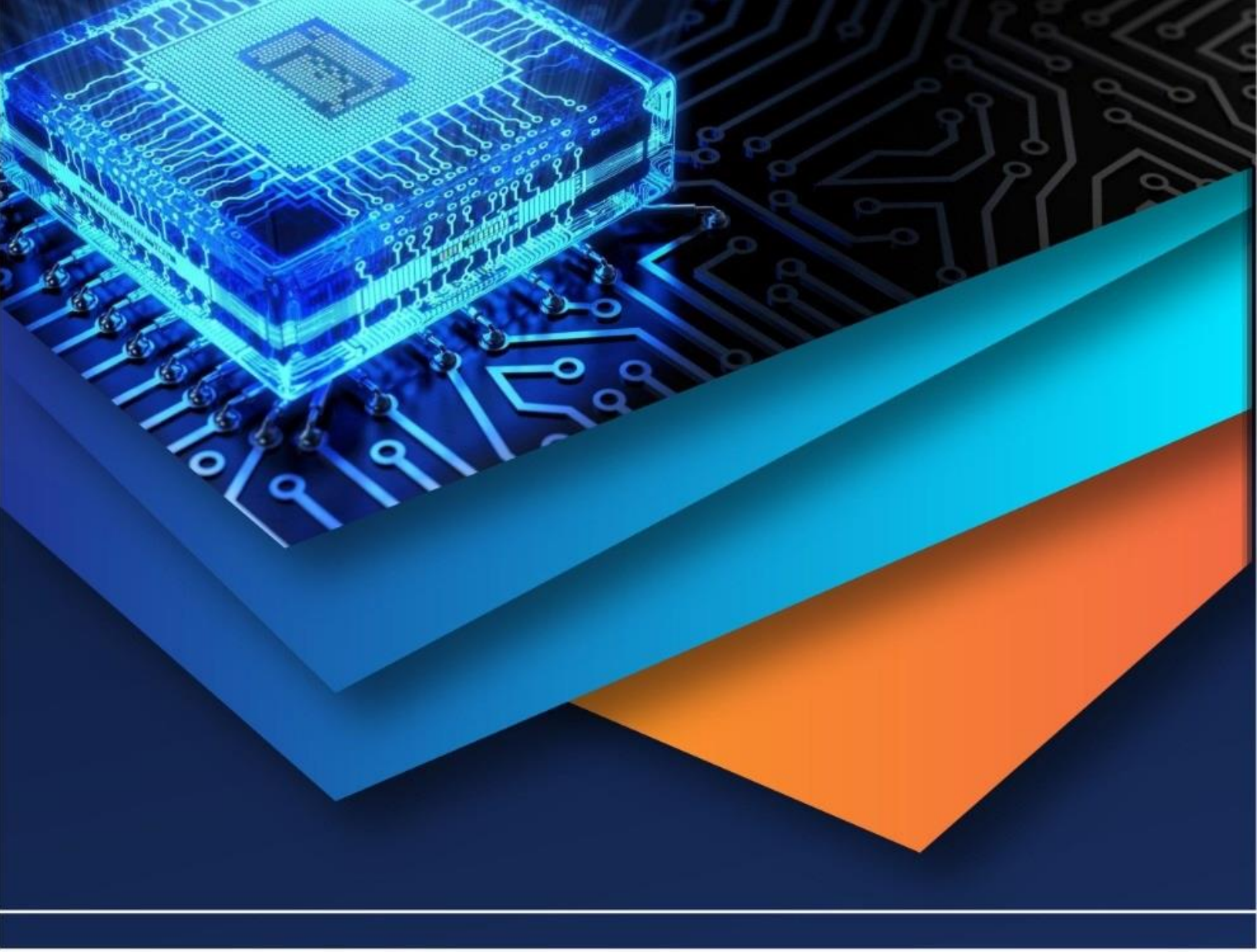

10.22214/IJRASET

45.98

IMPACT FACTOR: 7.129

IMPACT FACTOR: 7.429

INTERNATIONAL JOURNAL FOR RESEARCH

IN APPLIED SCIENCE & ENGINEERING TECHNOLOGY